Research Article | Vol. 27, No. 11 | 27 May 2019 | OPTICS EXPRESS 15693
Optics EXPRESS

Excessively tilted fiber grating based Fe_3O_4 saturable absorber for passively mode-locked fiber laser

HUSHAN WANG,[1,2,3,6] FENGYAN ZHAO,[1,2,3,6] ZHIJUN YAN,[1,4] XIAOHONG HU,[1] KAIMING ZHOU,[1,5] TING ZHANG,[1,2] WEI ZHANG,[1] YISHAN WANG,[1,3,7] WEI ZHAO,[1,3,8] LIN ZHANG,[5] AND CHUANDONG SUN[1]

[1]*State Key Laboratory of Transient Optics and Photonics, Xi'an Institute of Optics and Precision Mechanics, Chinese Academy of Sciences, Xi'an 710119, China*
[2]*University of Chinese Academy of Sciences, Beijing 10049, China*
[3]*Collaborative Innovation Center of Extreme Optics, Shanxi University, Taiyuan 030006, China*
[4]*The School of Optical and Electronic Information, National Engineering Laboratory for Next Generation Internet Access System, Huazhong University of Science and Technology, Wuhan 430074, Hubei, China*
[5]*Institute of Photonic Technologies, Aston University, Birmingham B4 7ET, UK*
[6]*These authors contributed equally to this work*
[7] *yshwang@opt.ac.cn*
[8] *weiz@opt.ac.cn*

Abstract: A novel approach to saturable absorber (SA) formation is presented by taking advantage of the mode coupling property of excessively tilted fiber grating (Ex-TFG). Stable mode-locked operation can be conveniently achieved based on the interaction between Ex-TFG coupled light and deposited ferroferric-oxide (Fe_3O_4) nanoparticles. The central wavelength, bandwidth and single pulse duration of the output are 1595 nm, 4.05 nm, and 912 fs, respectively. The fiber laser exhibits good long-term stability with signal-to-noise ratio (SNR) of 67 dB. For the first time, to the best of our knowledge, Ex-TFG based Fe_3O_4 SA for mode-locked fiber laser is demonstrated.

1. Introduction

Stable ultrashort pulse fiber lasers are of great importance for many fields in science and engineering, such as optical communication, laser material processing and biomedical optics. In the process of mode-locking initiation and ultrashort pulse generation, SAs play a key role. In the meantime, SAs also determine the pulse energy and stability of the fiber laser. Therefore, great efforts have been devoted to improving the properties of SAs in the recent decade. Compared with artificial SAs such as nonlinear polarization rotation (NPR) [1] and nonlinear optical loop mirror (NOLM) [2], real SAs have higher environmental persistence. For the sake of enhancing power resistance, these SAs have evolved from traditional semiconductor saturable absorber mirrors (SESAMs) [3] to one-dimensional and two-dimensional materials, such as carbon nanotubes [4–6], graphene [7–11], black phosphorous [12–15], and transition-metal dichalcogenides (TMDs) [16–20]. Quite recently, it has been demonstrated that another novel material group of zero-dimension transition metal oxides (TMOs) including TiO_2, ZnO, Al_2O_3 and Fe_3O_4 possesses efficient nonlinear SA properties [21–28]. Compared with carbon nanotubes and other two-dimension materials, the prepared zero-dimension nanomaterials-based SA is more uniform due to their smaller lateral size and regular circle-like shape [24–26]. Among the TMOs, Fe_3O_4 is an attractive nanomaterial due to large third-order nonlinear susceptibility of 4.0×10^{-10} esu and a high nonlinear optical absorption. Besides, Fe_3O_4 nanoparticles possess semiconductors property, fast response time ranging from 18 to 30 picoseconds and tunable bandgap [24]. In 2016, Bai et al. verified the

#364692 https://doi.org/10.1364/OE.27.015693
Journal © 2019 Received 9 Apr 2019; revised 9 May 2019; accepted 9 May 2019; published 17 May 2019

Optics EXPRESS

nonlinear optical response characteristic of Fe_3O_4 nanoparticles and realized a passively Q-switching operation in erbium-doped fiber laser [25]. Subsequently, Mao et al. fabricated two filmy Fe_3O_4 SAs by mixing Fe_3O_4 nanoparticles into the polyvinyl alcohol solution and polyimide solution to obtain Q-switching operation at 1.55 μm [26]. However, for the moment, there are still no reports on stable mode-locked operation in fiber lasers by using the Fe_3O_4 based SA.

The interaction between nanomaterials and propagating wave in the fiber laser is the key of realizing an effect SA. One common method is applying optical devices with special physical structure that can leak out a fraction of laser field which propagates in the form of evanescent wave. Researchers have focused on tapered-fibers [29,30], D-shaped fibers [31,32], fiber microchannels [33,34] and hollow-core fibers [35]. All these devices have been proved to be effective schemes for integration and employed in most SAs. Nonetheless, their limitations still exist. The realization of D-shaped fibers and nanomaterials-filled fiber microchannels requires complex technology and expensive equipments. The tapered-fibers are easy to break due to the small waist diameter. The hollow-core fibers have complicated structure and needs hard fusion process.

Ex-TFGs with tilted angle over 70 degrees possess typical polarization characters and can realize forward mode coupling [36,37]. These gratings have been applied in various domains including signal processing, optical communication, fiber lasers and sensors [38–42]. Considering the radiation property of Ex-TFGs, it turns out to be a feasible solution to realize SA mechanism via coating Ex-TFGs with nanomaterials. Meanwhile, the SA can have multiple significant advantages benefiting from the following properties of Ex-TFG: the Ex-TFG with relatively long length and large surface area can facilitate the interaction between the coupled light and deposited materials; the leaking-out light power from Ex-TFG can be adjusted through polarization control, which contributes to the balance of gain and loss in the cavity; the Ex-TFG has function of filtering and can easily control the mode-locking waveband and suppress mode competition; the Ex-TFG inscribed in normal single mode fiber (SMF) has high reliability without any splicing problem or extra loss.

In this work, the Ex-TFG is introduced into SA schemes for the first time. By depositing liquid phase exfoliated Fe_3O_4 nanoparticles onto an Ex-TFG, we realize a practical SA for fiber lasers. It is also the first time, to the best of our knowledge, that stable mode-locked operation is achieved in a fiber laser based on Fe_3O_4. Owing to the merits of Ex-TFG and Fe_3O_4, the SNR of the radio frequency spectrum can reach 67 dB and the fiber laser exhibits high stability.

2. Fabrication and characterization of deposited Ex-TFG based Fe_3O_4 SA

We use liquid phase exfoliated method to fabricate Fe_3O_4 nanoparticles SA. Fe_3O_4 nanoparticles are dispersed in N-Methylpyrrolidone (NMP) solution with a concentration of 0.3 mg/ml. The mixture is placed in a high power ultrasonic cleaner (40 kHz frequency, 55-60°C temperature and 360 W ultrasonic power) for 10 hours to form uniform suspension. The prepared Fe_3O_4 solution presents rust brown color, as shown in Fig. 1(a). The scanning electron microscope (SEM) image of Fe_3O_4 nanoparticles is recorded in Fig. 1(b). The Fe_3O_4 nanoparticles present uniform spherical shape. The lateral sizes of the most of nanoparticales vary approximately from 54 nm to 300 nm, which are larger than the original Fe_3O_4 nanoparticles with an average diameter of 54 nm. It is attributed to the NMP coated film and random agglomeration of Fe_3O_4 nanoparticles when prepared suspension is exposed in air. The bandgap of the Fe_3O_4 nanoparticles is designed to be 0.3 eV, which means that the material can be operated well in the wavelength region below 4.1 μm. The transmittance of the Fe_3O_4 nanoparticles is measured by a Fourier transform infrared spectrometer (Bruker VERTEX 80/80v). It can be seen from Fig. 1(c) that the material displays a broadband linear absorption property and the transmission of the material is about 35.6% at 1595 nm. According to the transmission spectrum, although the absorption is weaker than that at other

Optics EXPRESS

wavebands, the material still has a relatively high linear absorption compared with some other SA materials, which is sufficient for initiating mode-locking [6,10,15,43]. The energy dispersive spectroscopy (EDS) spectrum of Fe_3O_4 nanoparticles is also measured, as shown in Fig. 1(d). Strong intensity peaks representing Fe and O are clearly observable, which matches well with the result of Fe_3O_4 nanoparticles [28]. In addition, C is the residual element of NMP solution, and Si and Al are derived from the silicon wafer and substrates of the measuring device.

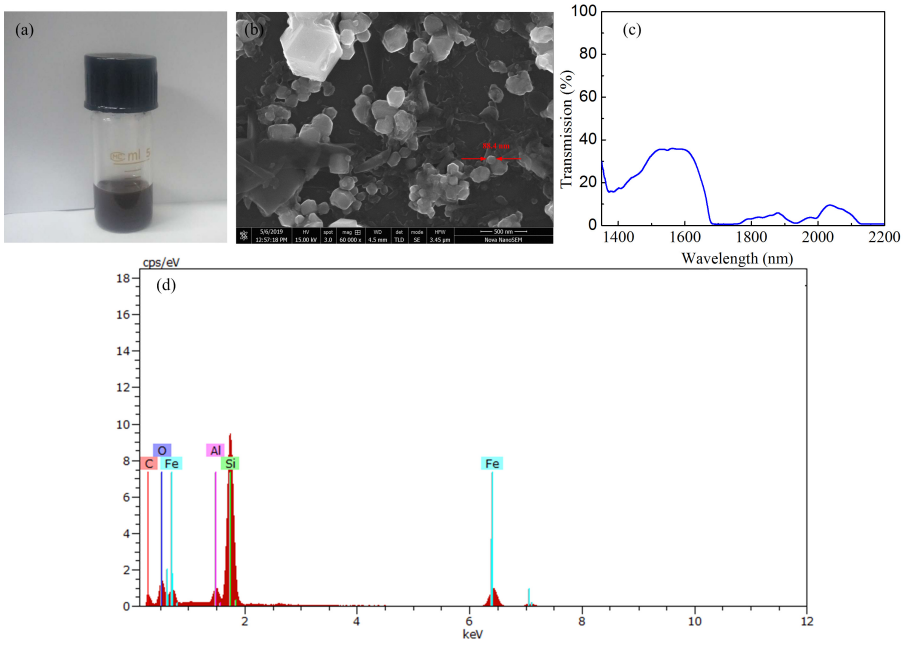

Fig. 1. (a) Photograph of uniform Fe_3O_4 nanoparticles suspension; (b) The SEM image, (c) the transmission and (d) the EDS spectrum of the Fe_3O_4 nanoparticles.

The Ex-TFG is inscribed in hydrogenated standard SMF by using typical scanning mask technique. A custom-designed amplitude mask with a period of 6.6 μm is utilized to ensure that grating responses are positioned in the C-L band. Due to the cylindrical geometry of fiber, the tilted angle of interference pattern inside the fiber is different with that outside the fiber [44]. In the UV inscription, the mask is tilted at 76° to induce tilted fringes at around 80.6° in the fiber. Besides, the grating has a relatively long length of around 10 mm, which benefits the interaction between the coupled light and materials.

The prepared uniform suspension of Fe_3O_4 nanoparticles is dropped onto the surface of the Ex-TFG by using a pipette, and then a continuous laser of approximately 91 mW power is injected into the Ex-TFG for the deposition by optical trapping effect. The deposition process lasts for over one hour to achieve the SA. The photograph of the SA is provided in Fig. 2(a) and it looks almost the same as normal fiber without coating by the naked eye. The micrograph is shown in Fig. 2(b), from which it can be clearly seen that the Fe_3O_4 nanoparticles are deposited on the grating. The operation principle of the Fe_3O_4 based Ex-TFG is illustrated in Fig. 2(c). The incident light is firstly coupled into cladding modes by Ex-TFG. As the Fe_3O_4 nanoparticles are directly deposited onto the surface of cladding with no gap, most coupled light can interact with the material through the evanescent field. The large surface area also contributes to the interaction. Then, the interacted light can be partially coupled back into the core mode by the Ex-TFG. The transmission spectra of the Ex-TFG deposited with Fe_3O_4 nanoparticles are shown in Fig. 3(a). With random polarization light, the typical dual peaks centered at 1599 nm and 1605 nm are coupled with almost the same

Optics EXPRESS

strength showing ~3 dB transmission loss. When it is switched to orthogonally polarized lights, one peak is almost diminished while the other is fully excited with about 5.6 dB attenuation, indicating 5.6 dB polarization extinction ratio (PER) of the Fe_3O_4 nanoparticles deposited Ex-TFG. The nonlinear transmission characteristic of this SA device is measured by using typical balanced twin-detector measurement technique [45]. The modulation depth (MD) is measured to be 2.46%, as illustrated in Fig. 3(b). The typical saturation function of this device is suitable for realizing effective mode-locking.

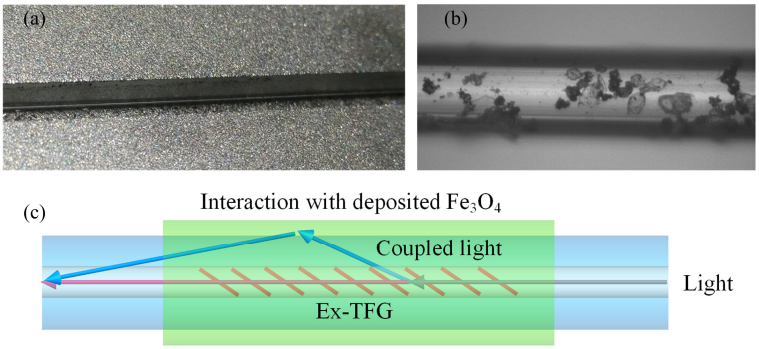

Fig. 2. (a) Photograph, (b) micrograph and (c) the operation principle illustration of Fe_3O_4 deposited Ex-TFG.

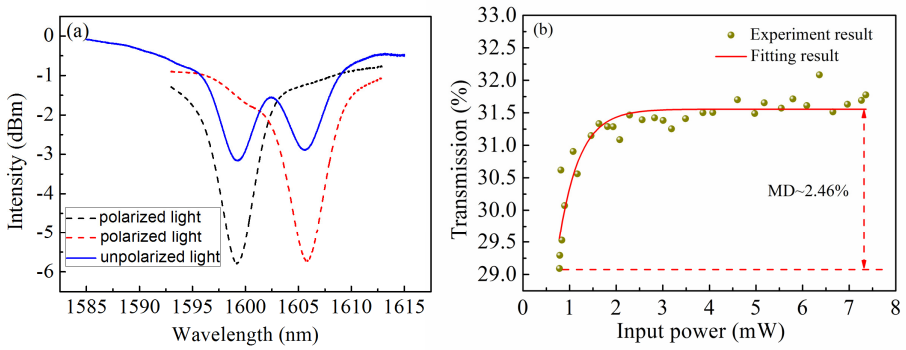

Fig. 3. (a) The transmission spectra of Fe_3O_4 coated Ex-TFG when launched with unpolarized light (blue line) and orthogonally polarized lights (red line and black line); (b) The nonlinear transmission curve of Fe_3O_4 coated Ex-TFG.

3. Experimental results and discussion

Based on the Fe_3O_4 nanoparticles deposited Ex-TFG, a pulsed erbium-doped fiber laser is built and the schematic diagram is shown in Fig. 4. The fiber laser is composed of 2.8 m erbium-doped fiber (EDF) (Nufern SM-ESF-7/125) with an absorption coefficient of 55 dB/m at 1530 nm, a polarization independent isolator (PI-ISO), Fe_3O_4 nanoparticles coated Ex-TFG as SA, two polarization controllers (PCs) and an optical coupler (OC) with an output ratio of 10%. A 980 nm laser diode (LD) providing up to 300 mW power pumps the cavity through a wavelength-division multiplexer (WDM). The total length of the cavity is about 13 m. The dispersion parameter of EDF and single mode fiber are –46.25 ps/nm/km and 18 ps/nm/km, respectively. The characteristics of mode locking pulses are recorded by an optical spectrum analyzer (Yokogawa AQ6370D), a digital oscillator (Tektronix TDS784D), a radio-frequency spectrum (Agilent technologies N9000A) and an autocorrelator (APE Pulse Check SM1200).

Optics EXPRESS

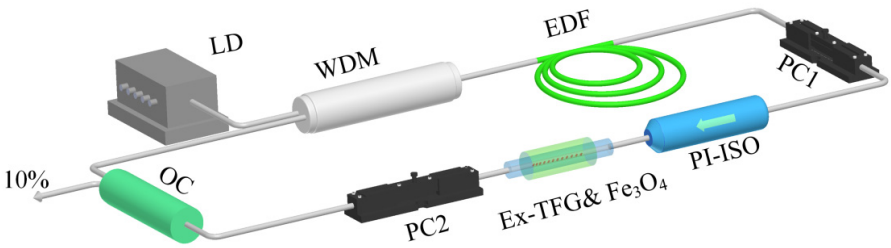

Fig. 4. The schematic diagram of mode-locked fiber laser by using Fe_3O_4 nanoparticles based Ex-TFG as the SA.

When the pump power is increased to 60 mW, single-pulse mode-locking is obtained by adjusting two PCs properly. On account of Fe_3O_4 nanoparticles with larger linear absorption compared with some other materials, the pump threshold is relatively high. When the incident pump power is beyond 200 mW, the fiber laser switches into multiple-pulse mode-locking. Figure 5(a) presents the variation of the output average power with the pump power in different mode-locking regimes. The output power varies monotonically with the increase of the incident pump power and the slope efficiency is 3.68%. Figure 5(b) presents the measured optical spectra corresponding to pump powers of 100 mW, 130 mW and 190 mW. The spectra are centered at around 1595 nm with 3 dB spectral bandwidth of 4.05 nm. It is worth noting that the centeral wavelength of mode-locked fiber laser dose not accord well with the coupling peak location of Ex-TFG. At 1595 nm, the coupling efficiency of Fe_3O_4 deposited Ex-TFG can be adjusted from 19.5% (0.94 dB) to 33.3% (1.76 dB) in theory, as shown in Fig. 3(a). Considering that over-high coupling strength may introduce great loss against mode-locking, it is believed that the coupling and gain are balanced at this wavelength and stable mode-locking operation is achieved. The result also indicates the advantage of the Ex-TFG with adjustable coupling efficiency. In the following, the properties of mode-locked pulses are recorded under 190 mW pump power. As displayed in Fig. 5(c), the pulse train exhibits uniform intensity and pulse-pulse interval of 63.1 ns which indicates a fundamental repetition frequency of 15.84 MHz. The pulse duration is measured by an autocorrelator and the autocorrelation trace is shown in Fig. 5(d). 912 fs single pulse duration is obtained when a $sech^2$ pulse profile is assumed. The time bandwidth product is 0.435 which approaches to the theoretical transform-limited value of 0.315. Meanwhile, the radio frequency spectrum is recorded to evaluate the stability of the fiber laser. Benefiting from the Fe_3O_4 deposited Ex-TFG, the SNR is greatly improved. The radio frequency spectrum presented in Fig. 5(e) exhibits the SNR up to 67 dB with the resolution bandwidth of 1 kHz, indicating a stable mode-locked operation. The inset shows the wideband radio frequency spectrum. The long-term stability of the mode-locked fiber laser is investigated as well. The spectrum of one mode-locking state is recorded every 30 minutes for a total lasting time of 8 hours. As exhibited in Fig. 5(f), the mode-locked state maintains stable and the spectrum of the fiber laser keeps almost unchanged with central wavelength shifting of 0.16 nm and power drifting of 1.2 dB.

In addition, we intentionally select the Ex-TFG with low PER to avoid NPR effect in the fiber laser. The maximal PER of Fe_3O_4 deposited Ex-TFG is only 5.6 dB and the PER is even less than 2 dB at the mode-locking central wavelength of 1595 nm. To initiate NPR mode-locking with such low PER in the fiber laser, high nonlinearity is needed which can be realized by using hundreds of meters long high nonlinear fibers and high pump power [42,46]. Considering that the cavity length in this experiment is only 13 m without any high nonlinear fibers and the mode-locking threshold is only 60 mW, it is not sufficient for initiating NPR mode-locking with the low PER. To verify this point of view, the Ex-TFG is firstly put into the same laser cavity without depositing any Fe_3O_4 nanoparticles. No mode-

Optics EXPRESS

locking indication can be observed even though two PCs are carefully adjusted with increasing pump power to the maximum value of 300 mW. Therefore, it suggests that the mode-locking operation purely depends on the interaction between the coupled light and Fe_3O_4 nanoparticles.

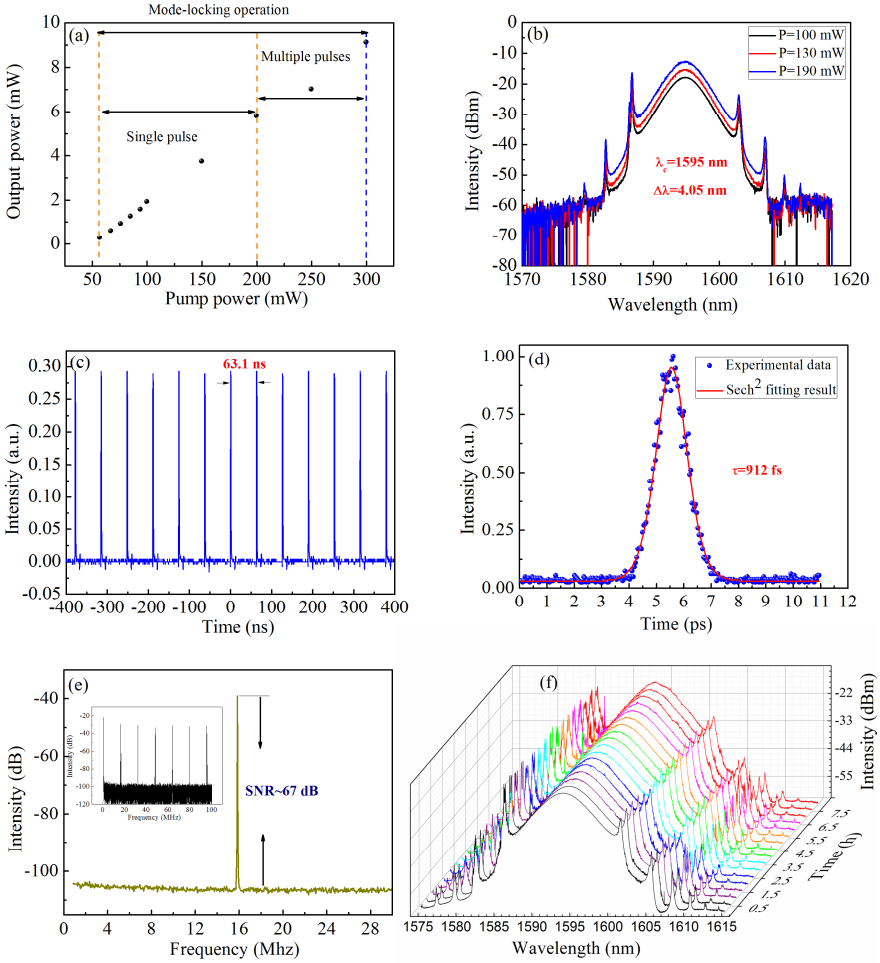

Fig. 5. Properties of the mode-locked fiber laser. (a) Output power as a function of incident pump power; (b) Optical spectra at different pump powers; (c) The waveform of the pulse train; (d) Autocorrelation trace; (e) Radio frequency spectrum of the fundamental repetition rate with inset showing the wideband radio frequency spectrum; (f) The long-term stability.

4. Conclusion

In summary, we have proposed and demonstrated the erbium-doped mode-locked fiber laser by using the interaction between the Ex-TFG with tilted angle of 80.6° and Fe_3O_4 nanoparticles. The modulation depth of the SA is measured to be 2.46%. The central wavelength and 3-dB bandwidth of spectrum are 1595 nm and 4.05 nm, respectively. The pulse duration of 912 fs is generated under a fundamental repetition frequency of 15.84 MHz. By employing Fe_3O_4 nanoparticles and Ex-TFG, the fiber laser shows good long-term stability with SNR up to 67 dB. Through this study, we provide a guideline for the design of Ex-TFG based SAs not only for Fe_3O_4 nanoparticles but also for all other nanomaterials.

Optics EXPRESS

Funding

National Natural Science Foundation of China (61605239, 61690222); National Key R & D Program of China (2016YFF0200700, 2017YFB1104400); CAS-SAFEA International Partnership Program for Creative Research Teams.

Acknowledgments

We are very grateful to Dr. Q. Abdul from Shaanxi Normal University for providing the Fe_3O_4 nanomaterials.

References

1. S. Wang, Z. Zhao, and Y. Kobayashi, "Wavelength-spacing controllable, dual-wavelength synchronously mode locked Er:fiber laser oscillator based on dual-branch nonlinear polarization rotation technique," Opt. Express **24**(25), 28228–28238 (2016).
2. Y. H. Zhong, Z. X. Zhang, and X. Y. Tao, "Passively mode-locked fiber laser based on nonlinear optical loop mirror with semiconductor optical amplifier," Laser Phys. **20**(8), 1756–1759 (2010).
3. L. Zhang, J. Zhou, Z. Wang, X. Gu, and Y. Feng, "SESAM mode-locked, environmentally stable, and compact dissipative soliton fiber laser," IEEE Photonics Technol. Lett. **26**(13), 1314–1316 (2014).
4. K. Wu, X. Li, Y. Wang, Q. J. Wang, P. P. Shum, and J. Chen, "Towards low timing phase noise operation in fiber lasers mode locked by graphene oxide and carbon nanotubes at 1.5 μm," Opt. Express **23**(1), 501–511 (2015).
5. W. S. Kwon, H. Lee, J. H. Kim, J. Choi, K. S. Kim, and S. Kim, "Ultrashort stretched-pulse L-band laser using carbon-nanotube saturable absorber," Opt. Express **23**(6), 7779–7785 (2015).
6. Y. W. Song, S. Yamashita, C. S. Goh, and S. Y. Set, "Carbon nanotube mode lockers with enhanced nonlinearity via evanescent field interaction in D-shaped fibers," Opt. Lett. **32**(2), 148–150 (2007).
7. Z. Luo, M. Zhou, J. Weng, G. Huang, H. Xu, C. Ye, and Z. Cai, "Graphene-based passively Q-switched dual-wavelength erbium-doped fiber laser," Opt. Lett. **35**(21), 3709–3711 (2010).
8. Z. Sun, T. Hasan, F. Torrisi, D. Popa, G. Privitera, F. Wang, F. Bonaccorso, D. M. Basko, and A. C. Ferrari, "Graphene mode-locked ultrafast laser," ACS Nano **4**(2), 803–810 (2010).
9. N. H. Park, H. Jeong, S. Y. Choi, M. H. Kim, F. Rotermund, and D. I. Yeom, "Monolayer graphene saturable absorbers with strongly enhanced evanescent-field interaction for ultrafast fiber laser mode-locking," Opt. Express **23**(15), 19806–19812 (2015).
10. B. Fu, Y. Hua, X. S. Xiao, H. W. Zhu, Z. P. Sun, and C. X. Yang, "Broadband Graphene Saturable Absorber for Pulsed Fiber Lasers at 1, 1.5, and 2 μm," IEEE J Sel. Top. Quant. **20**(5), 1100705 (2014).
11. H. R. Mu, Z. T. Wang, J. Yuan, S. Xiao, C. Y. Chen, Y. Chen, Y. Yao, J. C. Song, Y. Z. Xue, H. Zhang, and Q. L. Bao, "Graphene-Bi_2Te_3 heterostructure as saturable absorber for short pulse generation," ACS Photonics **2**(7), 832–841 (2015).
12. Y. Chen, S. Chen, J. Liu, Y. Gao, and W. Zhang, "Sub-300 femtosecond soliton tunable fiber laser with all-anomalous dispersion passively mode locked by black phosphorus," Opt. Express **24**(12), 13316–13324 (2016).
13. Z. C. Luo, M. Liu, Z. N. Guo, X. F. Jiang, A. P. Luo, C. J. Zhao, X. F. Yu, W. C. Xu, and H. Zhang, "Microfiber-based few-layer black phosphorus saturable absorber for ultra-fast fiber laser," Opt. Express **23**(15), 20030–20039 (2015).
14. Z. N. Guo, H. Zhang, S. B. Lu, Z. T. Wang, S. Y. Tang, J. D. Shao, Z. B. Sun, H. H. Xie, H. Y. Wang, X. F. Yu, and P. K. Chu, "From black phosphorus to phosphorene: basic solvent exfoliation, evolution of raman scattering, and applications to ultrafast photonics," Adv. Funct. Mater. **25**(45), 6996–7002 (2015).
15. J. Sotor, G. Sobon, W. Macherzynski, P. Paletko, and K. M. Abramski, "Black phosphorus saturable absorber for ultrashort pulse generation," Appl. Phys. Lett. **107**(5), 051108 (2015).
16. D. Mao, Y. Wang, C. Ma, L. Han, B. Jiang, X. Gan, S. Hua, W. Zhang, T. Mei, and J. Zhao, "WS_2 mode-locked ultrafast fiber laser," Sci. Rep. **5**(1), 7965 (2015).
17. K. Wu, X. Zhang, J. Wang, X. Li, and J. Chen, "WS□ as a saturable absorber for ultrafast photonic applications of mode-locked and Q-switched lasers," Opt. Express **23**(9), 11453–11461 (2015).
18. W. Liu, L. Pang, H. Han, M. Liu, M. Lei, S. Fang, H. Teng, and Z. Wei, "Tungsten disulfide saturable absorbers for 67 fs mode-locked erbium-doped fiber lasers," Opt. Express **25**(3), 2950–2959 (2017).
19. H. Zhang, S. B. Lu, J. Zheng, J. Du, S. C. Wen, D. Y. Tang, and K. P. Loh, "Molybdenum disulfide (MoS□) as a broadband saturable absorber for ultra-fast photonics," Opt. Express **22**(6), 7249–7260 (2014).
20. R. Khazaeizhad, S. H. Kassani, H. Jeong, D. I. Yeom, and K. Oh, "Mode-locking of Er-doped fiber laser using a multilayer MoS_2 thin film as a saturable absorber in both anomalous and normal dispersion regimes," Opt. Express **22**(19), 23732–23742 (2014).
21. H. Ahmad, S. A. Reduan, Z. A. Ali, M. A. Ismail, N. E. Ruslan, C. S. J. Lee, R. Puteh, and S. W. Harun, "C-band Q-switched fiber laser using titanium dioxide (TiO_2) as saturable absorber," IEEE Photonics J. **8**(1), 1 (2016).
22. H. Ahmad, C. S. J. Lee, M. A. Ismail, Z. A. Ali, S. A. Reduan, N. E. Ruslan, and S. W. Harun, "Tunable Q-switched fiber laser using zinc oxide nanoparticles as a saturable absorber," Appl. Opt. **55**(16), 4277–4281

Optics EXPRESS

(2016).
23. S. K. M. Al-Hayali, D. Z. Mohammed, W. A. Khaleel, and A. H. Al-Janabi, "Aluminum oxide nanoparticles as saturable absorber for C-band passively Q-switched fiber laser," Appl. Opt. **56**(16), 4720–4726 (2017).
24. X. Wang, Y. G. Wang, D. Mao, L. Li, and Z. D. Chen, "Passively Q-switched Nd:YVO_4 laser based on Fe_3O_4 nanoparticles saturable absorber," Opt. Mater. Express **7**(8), 2913–2921 (2017).
25. X. K. Bai, C. B. Mou, L. X. Xu, T. Y. Wang, S. L. Pu, and X. L. Zeng, "Passively Q-switched Erbium-doped fiber laser using Fe_3O_4-nanoparticle saturable absorber," Appl. Phys. Express **9**(4), 042701 (2016).
26. D. Mao, X. Q. Cui, W. D. Zhang, M. K. Li, T. X. Feng, B. B. Du, H. Lu, and J. L. Zhao, "Q-switched fiber laser based on saturable absorption of ferroferric-oxide nanoparticles," Photon. Res. **5**(1), 52–56 (2017).
27. Y. S. Chen, J. D. Yin, H. Chen, J. Z. Wang, P. G. Yan, and S. C. Ruan, "Single-Wavelength and Multiwavelength Q-switched Fiber Laser Using Fe_3O_4 Nanoparticles," IEEE Photonics J. **9**(2), 1 (2017).
28. J. Koo, J. Lee, J. Kim, and J. H. Lee, "A Q-switched, 1.89 μm fiber laser using an Fe_3O_4-based saturable absorber," J. Lumin. **195**, 181–186 (2018).
29. A. Martinez, M. A. Araimi, A. Dmitriev, P. Lutsyk, S. Li, C. B. Mou, A. Rozhin, M. Sumetsky, and S. Turitsyn, "Low-loss saturable absorbers based on tapered fibers embedded in carbon nanotube/polymer composites," APL Photonics **2**(12), 126103 (2017).
30. Y. W. Song, K. Morimune, S. Y. Set, and S. Yamashita, "Polarization insensitive all-fiber mode-lockers functioned by carbon nanotubes deposited onto tapered fibers," Appl. Phys. Lett. **90**(2), 021101 (2007).
31. E. J. Aiub, D. Steinberg, E. A. Thoroh de Souza, and L. A. M. Saito, "200-fs mode-locked Erbium-doped fiber laser by using mechanically exfoliated MoS₂ saturable absorber onto D-shaped optical fiber," Opt. Express **25**(9), 10546–10552 (2017).
32. D. Steinberg, J. D. Zapata, E. A. Thoroh de Souza, and L. A. M. Saito, "Mechanically exfoliated graphite onto d-shaped optical fiber for femtosecond mode-locked erbium-doped fiber laser," J. Lightwave Technol. **36**(10), 1868–1874 (2018).
33. K. Kashiwagi and S. Yamashita, "Deposition of carbon nanotubes around microfiber via evanascent light," Opt. Express **17**(20), 18364–18370 (2009).
34. A. Martinez, K. Zhou, I. Bennion, and S. Yamashita, "In-fiber microchannel device filled with a carbon nanotube dispersion for passive mode-lock lasing," Opt. Express **16**(20), 15425–15430 (2008).
35. S. Y. Choi, F. Rotermund, H. Jung, K. Oh, and D. I. Yeom, "Femtosecond mode-locked fiber laser employing a hollow optical fiber filled with carbon nanotube dispersion as saturable absorber," Opt. Express **17**(24), 21788–21793 (2009).
36. Z. Yan, H. Wang, C. Wang, Z. Sun, G. Yin, K. Zhou, Y. Wang, W. Zhao, and L. Zhang, "Theoretical and experimental analysis of excessively tilted fiber gratings," Opt. Express **24**(11), 12107–12115 (2016).
37. K. Zhou, L. Zhang, X. Chen, and I. Bennion, "Optic sensors of high refractive-index responsivity and low thermal cross sensitivity that use fiber Bragg gratings of >80 ° tilted structures," Opt. Lett. **31**(9), 1193–1195 (2006).
38. B. Q. Jiang, K. M. Zhou, C. L. Wang, Q. Z. Sun, G. L. Yin, Z. J. Tai, K. Wilson, J. L. Zhao, and L. Zhang, "Label-free glucose biosensor based on enzymatic graphene oxide-functionalized tilted fiber grating," Sens. Actuators B Chem. **254**, 1033–1039 (2018).
39. B. Jiang, K. Zhou, C. Wang, Y. Zhao, J. Zhao, and L. Zhang, "Temperature-calibrated high-precision refractometer using a tilted fiber Bragg grating," Opt. Express **25**(21), 25910–25918 (2017).
40. Z. Yan, Q. Sun, C. Wang, Z. Sun, C. Mou, K. Zhou, D. Liu, and L. Zhang, "Refractive index and temperature sensitivity characterization of excessively tilted fiber grating," Opt. Express **25**(4), 3336–3346 (2017).
41. Z. J. Yan, Z. Y. Sun, K. M. Zhou, B. B. Luo, J. F. Li, H. S. Wang, Y. S. Wang, W. Zhao, and L. Zhang, "Numerical and experimental analysis of sensitivity-enhanced RI sensor based on Ex-TFG in thin cladding Fiber," J. Lightwave Technol. **33**(14), 3023–3027 (2015).
42. Z. Zhang, C. Mou, Z. Yan, Y. Wang, K. Zhou, and L. Zhang, "Switchable dual-wavelength Q-switched and mode-locked fiber lasers using a large-angle tilted fiber grating," Opt. Express **23**(2), 1353–1360 (2015).
43. Q. Wu, S. Chen, Y. Z. Wang, L. M. Wu, X. T. Jiang, F. Zhang, X. X. Jin, Q. Y. Jiang, Z. Zheng, J. Q. Li, M. Zhang, and H. Zhang, "MZI-based all-optical modulator using MXene $Ti_3C_2T_X$ (T=F, O, or OH) deposited microfiber," Adv. Mater. Technol. **4**(4), 1800532 (2019).
44. S. J. Mihailov, R. B. Walker, P. Lu, H. Ding, X. Dai, C. Smelser, and L. Chen, "UV-Induced polarization-dependent loss (PDL) in tilted fiber Bragg grating: Application of a PDL equalizer," IEE Proc., Optoelectron. **149**(5), 211–216 (2002).
45. J. M. Liu, Y. Chen, Y. Li, H. Zhang, S. Q. Zheng, and S. X. Xu, "Switchable dual-wavelength Q-switched fiber laser using multilayer black phosphorus as a saturable absorber," Photon. Res. **6**(3), 198–203 (2018).
46. T. X. Wang, Z. J. Yan, Q. Q. Huang, C. H. Zou, C. B. Mou, K. M. Zhou, and L. Zhang, "Mode-locked erbium-doped fiber lasers using 45° tilted fiber grating," IEEE J. Sel. Top. Quant. **24**(3), 1 (2018).